Bryostatin-1 alleviates experimental multiple sclerosis

Michael D. Kornberg[a], Matthew D. Smith[a], Hasti Atashi Shirazi[b], Peter A. Calabresi[a,c], Solomon H. Snyder[b,c,d,1], and Paul M. Kim[b,1]

[a]Department of Neurology, Johns Hopkins University School of Medicine, Baltimore, MD 21287; [b]Department of Psychiatry and Behavioral Sciences, Johns Hopkins University School of Medicine, Baltimore, MD 21287; [c]Department of Neuroscience, Johns Hopkins University School of Medicine, Baltimore, MD 21205; and [d]Department of Pharmacology and Molecular Sciences, Johns Hopkins University School of Medicine, Baltimore, MD 21205

Contributed by Solomon H. Snyder, January 3, 2018 (sent for review November 27, 2017; reviewed by Anne B. Young and Scott S. Zamvil)

Multiple sclerosis (MS) is an inflammatory disorder targeting the central nervous system (CNS). The relapsing-remitting phase of MS is largely driven by peripheral activation of autoreactive T-helper (Th) 1 and Th17 lymphocytes. In contrast, compartmentalized inflammation within the CNS, including diffuse activation of innate myeloid cells, characterizes the progressive phase of MS, the most debilitating phase that currently lacks satisfactory treatments. Recently, bryostatin-1 (bryo-1), a naturally occurring, CNS-permeable compound with a favorable safety profile in humans, has been shown to act on antigen-presenting cells to promote differentiation of lymphocytes into Th2 cells, an action that might benefit Th1-driven inflammatory conditions such as MS. In the present study, we show that bryo-1 provides marked benefit in mice with experimental autoimmune encephalomyelitis (EAE), an experimental MS animal model. Preventive treatment with bryo-1 abolishes the onset of neurologic deficits in EAE. More strikingly, bryo-1 reverses neurologic deficits after EAE onset, even when treatment is initiated at a late stage of disease when peak adaptive immunity has subsided. Treatment with bryo-1 in vitro promotes an anti-inflammatory phenotype in antigen-presenting dendritic cells, macrophages, and to a lesser extent, lymphocytes. These findings suggest the potential for bryo-1 as a therapeutic agent in MS, particularly given its established clinical safety. Furthermore, the benefit of bryo-1, even in late treatment of EAE, combined with its targeting of innate myeloid cells suggests therapeutic potential in progressive forms of MS.

multiple sclerosis | EAE | bryostatin | neuroimmunology

Bryostatin-1 (bryo-1) is a naturally occurring macrocyclic lactone obtained from the marine bryozoan *Bugula neritina* (1). It has shown clinical promise in cancer and Alzheimer's disease models based on its actions on protein kinase C and has proceeded through phase 2 clinical trials in humans with a favorable safety profile (2–9). Bryo-1 can also affect the immune system by modulating dendritic cells (DCs) via toll-like receptor 4 (TLR4) through the MyD88-independent pathway, which favors an anti-inflammatory environment by inducing a type 2 phenotype that promotes the differentiation of $CD4^+$ T-helper (Th) lymphocytes into Th2 versus Th1 effector cells (10–13). Such actions might be expected to favorably influence Th1-driven inflammatory conditions such as multiple sclerosis (MS) (14).

MS is an inflammatory disease of the central nervous system (CNS) that primarily targets oligodendrocytes and causes demyelination, although neurodegeneration is also a feature of the disease, particularly in its late stages (15). In most patients (~85–90%), early disease is characterized by acute episodes of focal inflammation causing neurologic disability, with intervening remission and at least partial recovery (termed relapsing-remitting MS, or RRMS). Subsequently, many patients with RRMS enter secondary progressive MS, which is characterized by progressive neurologic disability despite a lack of episodic relapses. Some patients (~10–15%) initially present with primary progressive MS and have a progressive course from the beginning with no history of episodic relapse. Although the most substantial disability develops during progressive MS, progressive forms of the disease have proven most difficult to treat, representing a major unmet need for patients with MS.

Distinct but overlapping immunologic mechanisms contribute to CNS injury in RRMS versus the progressive forms of disease (primary progressive MS and secondary progressive MS). The inflammatory plaques of RRMS are composed largely of Th cells, with evidence suggesting Th1 and Th17 effector subsets play a pathogenic, proinflammatory role, whereas Th2 and regulatory T cells modulate the immune response in a protective manner (16). Autoreactive Th cells are activated and polarized to distinct subsets in the periphery by antigen-presenting cells (APCs) such as DCs. They then track to the CNS, where they are restimulated by local myeloid cells including DCs, macrophages, and microglia. In progressive forms of MS, in contrast, dense lymphocytic infiltrates no longer exist, but innate myeloid cell activation continues both at the edges of slowly expanding plaques and more diffusely throughout the white and gray matter (17).

Experimental autoimmune encephalomyelitis (EAE) is a widely employed experimental animal model that recapitulates some aspects of MS. In the active-induction model of mouse EAE, mice are immunized with a peptide derived from myelin oligodendrocyte glycoprotein ($MOG_{35–55}$), resulting in robust CNS inflammation causing demyelination, axonal injury, and motor weakness/paralysis. EAE has proven very useful in elucidating key immunologic events relevant to MS, as well as in MS drug development (18, 19).

Based on its previously published effects on DCs via modulation of TLR4, which would be expected to inhibit differentiation

Significance

Multiple sclerosis (MS) is an inflammatory disease that targets the central nervous system and leads to severe neurologic disability. Bryostatin-1 is a naturally occurring, brain-penetrant compound that has undergone human testing in cancer and Alzheimer's disease, but also has immunomodulatory properties that might provide benefit in MS. Here, we show that bryostatin-1 potently prevents disease and reverses neurologic deficits in the major mouse model of MS, experimental autoimmune encephalomyelitis (EAE). Its benefit even in late-stage EAE further suggests potential in progressive forms of MS, in which much disability accrues but treatments are currently lacking. The established clinical safety profile of bryostatin-1 in humans could expedite its development as a therapeutic agent in MS.

Author contributions: M.D.K., M.D.S., P.A.C., S.H.S., and P.M.K. designed research; M.D.K., M.D.S., H.A.S., and P.M.K. performed research; P.A.C. contributed new reagents/analytic tools; M.D.K., M.D.S., H.A.S., P.A.C., S.H.S., and P.M.K. analyzed data; and M.D.K., M.D.S., P.A.C., S.H.S., and P.M.K. wrote the paper.

Reviewers: A.B.Y., Massachusetts General Hospital and Harvard Medical School; and S.S.Z., University of California, San Francisco.

The authors declare no conflict of interest.

[1]To whom correspondence may be addressed. Email: ssnyder@jhmi.edu or pmkim@jhmi.edu.

Published online February 12, 2018.

of pathogenic Th1 cells, we hypothesized that bryo-1 would have a therapeutic role in MS and EAE. In the present study, we demonstrate dramatic beneficial effects of bryo-1 in EAE with high potency, whether administered concurrently with $MOG_{35–55}$ immunization or up to as late as 28 d postimmunization. Although we observed direct effects of bryo-1 on T cells, the most potent in vitro effects were on DCs and macrophages. Our results suggest a possible role for bryo-1 in MS treatment. Moreover, the benefit seen in late treatment of EAE combined with its anti-inflammatory effects on macrophages suggests therapeutic potential in progressive forms of MS, for which treatment options are currently lacking.

Results

Bryo-1 Prevents the Induction of EAE. We elicited EAE by immunizing 8–12-wk-old C57BL/6J mice with $MOG_{35–55}$. Neurologic symptoms of EAE were most evident 10–14 d after MOG immunization, peaking at about 16 d and then plateauing with slight diminution until 21 d. Mice were treated with bryo-1 (30 μg/kg) or vehicle by i.p. injection 3 d per week. This dosing regimen was chosen based on previous work in an Alzheimer's mouse model (5). In initial experiments, treatment began on the day of $MOG_{35–55}$ immunization (day 0). In this prevention paradigm, bryo-1 treatment abolished the onset of EAE (Fig. 1*A*), suggesting that bryo-1 prevents the pathogenic peripheral immune response to $MOG_{35–55}$ immunization. Consistent with this hypothesis, flow cytometry from lymph nodes 8 d after immunization revealed significantly decreased numbers of total $CD4^+$ ($CD3^+$;$CD4^+$), Th1 ($CD4^+$;$IFN\gamma^+$), and Th17 ($CD4^+$;$IL17^+$) lymphocytes with bryo-1 treatment (Fig. 1*B*). Among $CD4^+$ lymphocytes, a significantly lower proportion of Th1 cells was observed with bryo-1 treatment, with a nonsignificant decrease in the proportion of Th17 cells (Fig. 1*C*). Similarly, flow cytometry from spleen at day 8 revealed significantly decreased numbers of total $CD4^+$ and Th1 lymphocytes with bryo-1 treatment, with a trend toward decreased Th17 cells (Fig. 1*D*).

Consistent with the diminished peripheral immune response, prophylactic bryo-1 led to diminished infiltration of $CD4^+$ lymphocytes into the brain (Fig. 1*E*) and spinal cord (Fig. 1*F*) at peak disease (day 14), with a decreased proportion of $CD4^+$ lymphocytes producing IFNγ. The percentage of infiltrating $CD4^+$ lymphocytes expressing IL17 was unchanged with bryo-1 treatment.

Bryo-1 Attenuates Neurologic Deficits in Established EAE. To further ascertain the potential clinical relevance of bryo-1, we explored its effects in two distinct therapeutic paradigms. In both paradigms, the treatments began after the onset of EAE, but the start of the treatments occurred at two different stages of the disease. In the first set of experiments, mice were randomized and treatment was initiated at the first clinical sign of motor weakness, corresponding to tail paralysis (Fig. 2*A*). As shown, bryo-1 substantially attenuated motor deficits and the subsequent course of EAE in this paradigm. Bryo-1-treated mice exhibited a lower peak clinical score and faster recovery than vehicle-treated mice. Flow cytometry from spinal cord at day 18 postimmunization (late peak), several days after initiating treatment, revealed significantly diminished numbers of Th1 and Th17 cells in bryo-1-treated mice, with a near-significant trend ($P = 0.06$) toward decreased total $CD4^+$ lymphocytes, suggesting faster resolution of CNS inflammation (Fig. 2*B*).

In another set of mice, to determine whether bryo-1 could reverse established neurologic deficits in EAE, we randomized mice and began treatment on day 28 postimmunization, more than 10 d after peak disease and once motor deficits had reached a stable plateau (Fig. 2*C*). Remarkably, bryo-1 reversed motor deficits even at this late stage of disease, with improvement observed within a week of treatment initiation. Treatment was continued for just more than 3 wk and discontinued on day 51 postimmunization. The clinical scores of bryo-1-treated mice steadily improved throughout the treatment period and for several days after discontinuation. Neurologic deficits worsened approximately 1 wk after discontinuing bryo-1, although interestingly, the clinical scores of these mice remained significantly lower than those of the vehicle-treated group.

Bryo-1 Promotes an Anti-Inflammatory Phenotype in APCs and Macrophages. The failure of bryo-1-treated mice to mount a pathogenic peripheral immune response to $MOG_{35–55}$ immunization during the prevention paradigm suggested a primary deficit in antigen presentation, consistent with prior reports of bryo-1's effects on antigen-presenting DCs (10). To further explore the effects of bryo-1 on APCs, we treated bone marrow-derived DCs (BMDCs) with bryo-1 in vitro, in the presence or absence of proinflammatory stimulation with lipopolysaccharide (LPS; Fig. 3). We first examined the effect of bryo-1 on expression of CD40 and CD86 via flow cytometry. CD40 is a costimulatory protein required for proinflammatory activation of APCs, whereas CD86 provides costimulatory activation of T cells upon their binding to APCs. Consistent with previous reports that bryo-1 alone can modulate DC effector function, we observed that bryo-1, even in the absence of LPS, up-regulates CD86, although it has no significant effect on CD40 in the absence of LPS (Fig. 3*A*). LPS alone markedly increased expression of both CD40 and CD86, but the LPS-induced up-regulation of CD40 was abrogated by simultaneous treatment with bryo-1 at either 20 or 200 nM. Bryo-1 had no effect on CD86 expression in LPS-stimulated BMDCs.

We next examined the effects of bryo-1 on cytokine secretion in LPS-stimulated BMDCs by ELISA (Fig. 3*B*). Low-dose bryo-1 (10 nM) abrogated LPS-induced secretion of IL-12, a proinflammatory cytokine that promotes Th1 differentiation. In contrast, bryo-1 significantly augmented secretion of IL-10, an anti-inflammatory cytokine that inhibits Th1 differentiation and promotes an immunoregulatory environment.

To explore the effects of bryo-1 on myeloid cells of the innate immune system, we used murine peritoneal macrophages (mPMs). Similar to its effect on dendritic cells, low-dose bryo-1 inhibited LPS-induced secretion of IL-12 and another proinflammatory cytokine, IL-6 (Fig. 3*C*). Furthermore, bryo-1 treatment of mPMs potentiated the IL-4-induced expression of arginase-1, a marker of the anti-inflammatory and repair-promoting M2 macrophage phenotype (Fig. 3*D*).

Direct Effects of Bryo-1 on T Cells. We also determined whether bryo-1 has direct influences on $CD4^+$ T cells in vitro that might be relevant to its observed benefit in EAE (Fig. 4). Although direct effects were observed in naive $CD4^+$ lymphocytes stimulated with α-CD3/CD28 antibodies, these effects were in general more modest than those observed in DCs, required higher doses of bryo-1, and were seen only with low levels of T-cell stimulation. Thus, bryo-1 treatment inhibited up-regulation of CD44 (a marker of T-cell activation; Fig. 4*A*) and IFNγ (Fig. 4*B*) and increased expression of the regulatory T-cell marker FoxP3 (Fig. 4*C*), but only at a dose of 200 nM in cells stimulated with 0.25 μg/mL of α-CD3 and α-CD28 antibodies. With stronger T-cell stimulation (1 μg/mL of α-CD3/CD28), these effects were lost.

Discussion

The most striking finding of this study is the marked beneficial effect of bryo-1 on EAE, whether administered concurrently with immunization, at the onset of neurologic signs, or as late as 28 d postimmunization, when the peak inflammatory phase has ended and neurologic disability has stabilized. This beneficial effect of bryo-1 occurs at a very low dose (30 μg/kg) administered only 3 d per week and is associated with broadly decreased inflammation both in the CNS and in the periphery, as assessed by flow

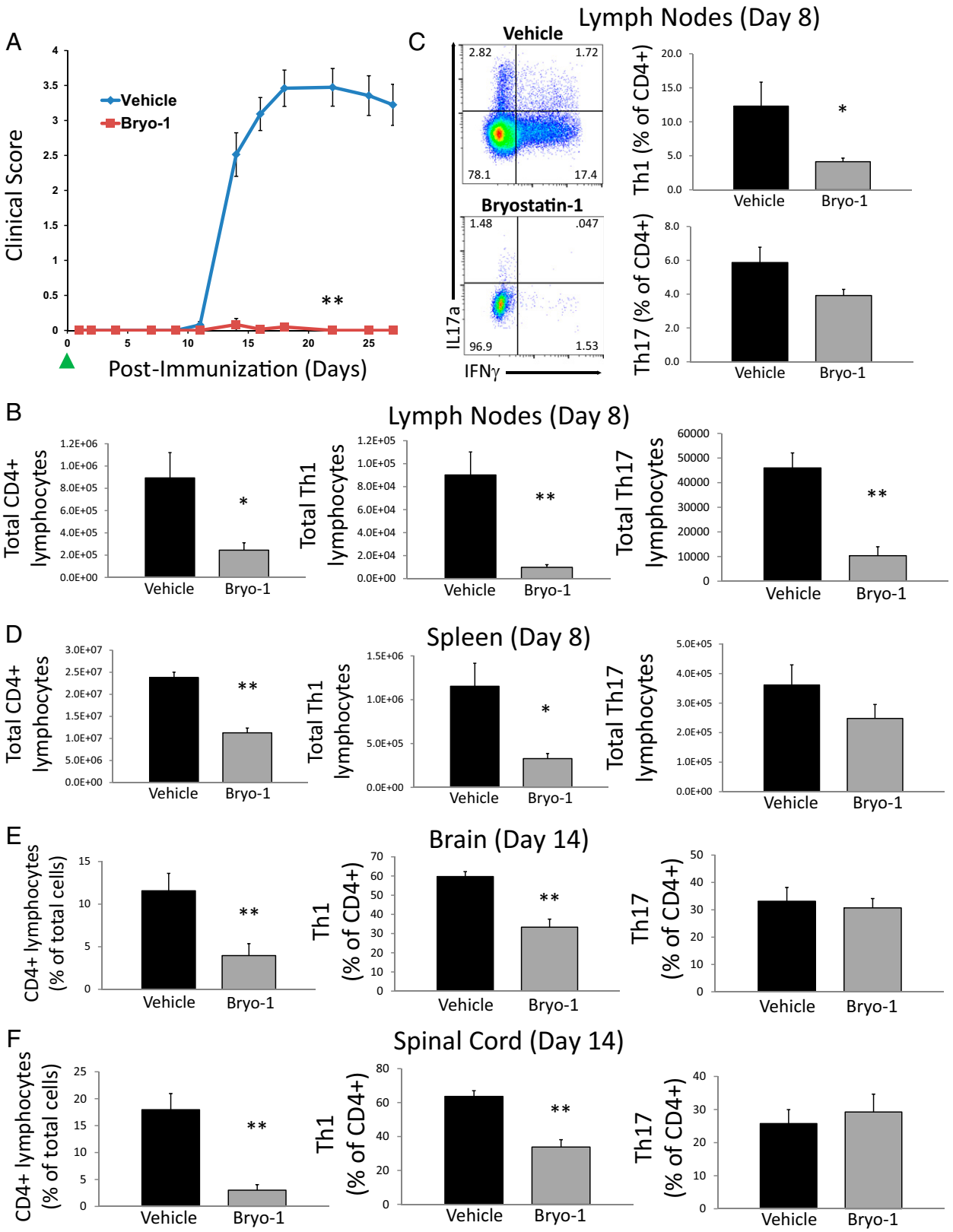

Fig. 1. Bryo-1 prevents the induction of EAE. (*A*) Clinical course of mice treated with bryo-1 (30 μg/kg) or vehicle alone by i.p. injection 3 d per week, beginning on the day of immunization with $MOG_{35–55}$ (day 0, green arrowhead); $n = 19$ and 15 mice in vehicle and bryo-1 groups, respectively. Error bars represent SEM. (*B* and *C*) Flow cytometry data from lymph nodes in EAE mice at day 8 postimmunization; $n = 5$ mice per group. (*B*) Total numbers of $CD4^+$ ($CD3^+$;$CD4^+$), Th1 ($CD4^+$;$IFN\gamma^+$), and Th17 ($CD4^+$;$IL17^+$) lymphocytes. (*C*) Proportion of Th1 and Th17 cells among $CD4^+$ lymphocytes, with representative flow plot. (*D*) Flow cytometry data from spleen in EAE mice (day 8), depicting total numbers of $CD4^+$, Th1, and Th17 lymphocytes; $n = 5$ mice per group. (*E* and *F*) Flow cytometry analysis of infiltrating $CD4^+$ lymphocytes in brain (*E*) and spinal cord (*F*) at peak EAE (day 14); $n = 9$ mice per group. All error bars represent SEM. Statistical significance was determined by Mann–Whitney *U* test for EAE clinical scoring and by two-tailed Student's *t* test for flow cytometry data (*$P < 0.05$; **$P < 0.01$).

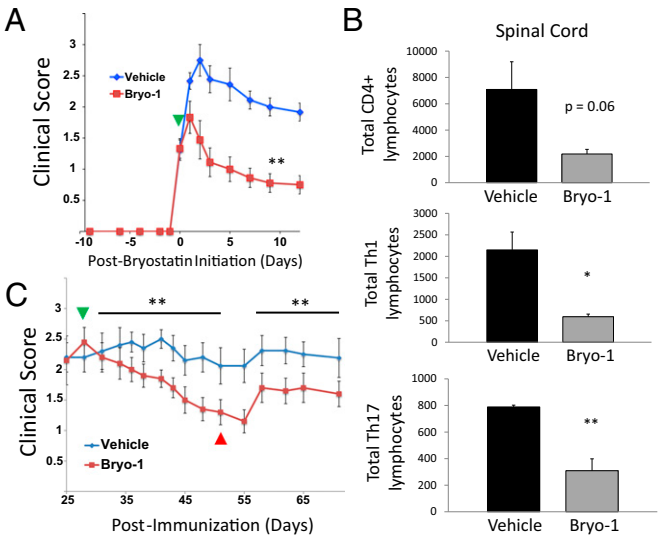

Fig. 2. Bryo-1 attenuates neurologic deficits and suppresses inflammation in established EAE. (*A*) EAE mice were randomized and treatment was initiated (green arrowhead) once they reached a clinical score of 1.0 (tail paralysis); $n = 9$ and 10 mice in vehicle and bryo-1 groups, respectively. (*B*) Flow cytometry analysis from spinal cord at day 18 postimmunization from EAE mice treated as in *A*. Data show total numbers of $CD4^+$, Th1, and Th17 lymphocytes. $n = 4$ mice per group. (*C*) EAE mice were randomized and treatment was initiated (green arrowhead) at day 28 postimmunization. Treatment was discontinued (red arrowhead) at day 51 postimmunization, and clinical course was followed through day 71; $n = 5$ mice per group. All error bars represent SEM. Statistical significance was determined by Mann–Whitney *U* test for EAE clinical scoring and by two-tailed Student's *t* test for flow cytometry data. (*C*) Curves were compared both before and after discontinuation-associated worsening (*$P < 0.05$; **$P < 0.01$).

cytometry. We find direct and potent (as low as 10 nM) anti-inflammatory effects of bryo-1 on DCs (as shown in previous reports) and macrophages. Finally, we also demonstrate direct effects of bryo-1 on $CD4^+$ T cells in vitro, albeit with much less potency.

Large numbers of agents prevent the development of EAE when treatment begins before or concurrent with immunization, but more limited numbers are effective when begun after immunologic priming has occurred and symptoms develop, which is more relevant to MS treatment in humans. Notably, currently treatments approved for MS by the U.S. Food and Drug Administration are effective in EAE in this therapeutic paradigm (19), providing promise that bryo-1 might be similarly effective in humans. Furthermore, although there is currently no well-established mouse model for progressive MS, the effectiveness of bryo-1 even at late-stage (day 28) EAE, after the acute phase and in the setting of a more smoldering-type inflammation, suggests potential for the heretofore elusive treatment of progressive disease characterized by compartmentalized CNS inflammation. The immunologic actions of bryo-1, a CNS-permeable compound, on macrophages support a potential role in treating compartmentalized innate immune activation, although effects on other relevant cell types (e.g., microglia) remain to be examined. Furthermore, the key molecular targets mediating its immunologic actions in EAE (e.g., protein kinase C vs. TLR4) remain to be elucidated.

One interesting finding from this study is that although discontinuation of bryo-1 at day 51 of the late-treatment paradigm led to a worsening of motor weakness, the clinical scores of these mice remained below those of vehicle-treated mice (Fig. 2*C*). It is interesting to speculate that this persistent improvement relative to vehicle-treated mice might represent stimulation of reparative/regenerative processes by bryo-1, possibly from the creation of a favorable immune environment. In this regard, we show here that bryo-1 treatment of mPMs inhibits classical activation and augments expression of the M2 marker arginase-1. In addition to the well-established role of M2 (or type II) monocytes in promoting a favorable profile of Th cell differentiation (14), M2 macrophages/microglia have been shown to promote oligodendrocyte differentiation during CNS remyelination (20). Furthermore, another TLR4 modulator, E6020, promotes remyelination in rat spinal cord by inducing macrophage phagocytosis of myelin debris (21). It is also notable that bryo-1 has been shown to have direct effects on OPCs, overcoming the inhibitory effects of myelin protein extracts on OPC differentiation (22).

Finally, the beneficial effects of bryo-1 on cognition and synaptogenesis that have been reported in mice (23–25) may have relevance in MS, as well. Cognitive deficits are common and often debilitating in MS, particularly in progressive phases of disease, yet no treatments targeting these deficits are available

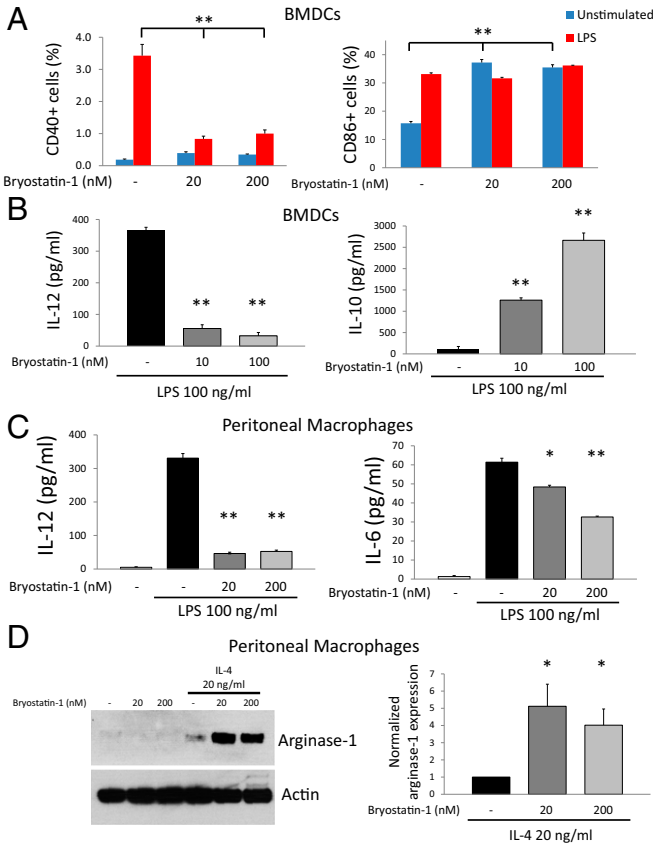

Fig. 3. Bryo-1 promotes an anti-inflammatory phenotype in APCs and macrophages. (*A*) BMDCs were treated overnight with the indicated doses of bryo-1, in the presence or absence of LPS (100 ng/mL). Expression of CD40 and CD86 was then determined by flow cytometry; $n = 3$ samples. (*B*) BMDCs were cotreated overnight with LPS and the indicated doses of bryo-1, and secretion of IL-12 and IL-10 into the culture media was measured via ELISA; $n = 2$ experiments performed in replicates of 4. (*C*) mPMs were cotreated overnight with LPS and the indicated doses of bryo-1, and secretion of IL-12 and IL-6 was measured via ELISA; $n = 2$ experiments performed in replicates of 4. (*D*) mPMs were treated with the indicated doses of bryo-1 overnight in the presence or absence of IL-4 (20 ng/mL), and the expression of arginase-1 was assessed by Western blot. (*D*, *Left*) Representative Western blot. (*Right*) Quantitation of arginase-1 Western blots from $n = 3$ experiments. All error bars represent SEM. Statistical analysis was performed using two-tailed Student's *t* test (*$P < 0.05$; **$P < 0.01$).

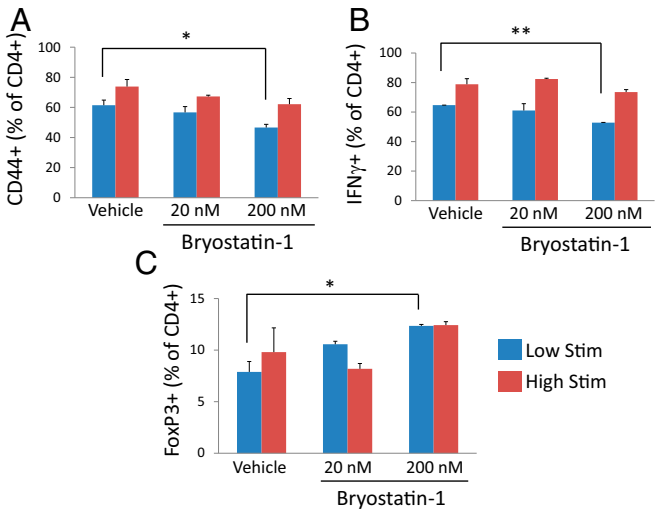

Fig. 4. Direct effects of bryo-1 on $CD4^+$ T-cells. Naive $CD4^+$ lymphocytes isolated by negative selection from mouse spleen were stimulated for 3 d with 0.25 μg/mL (low stim) or 1 μg/mL (high stim) each of α-CD3 and α-CD28 antibodies, along with the indicated concentrations of bryo-1. The percentages of $CD4^+$ lymphocytes expressing CD44 (*A*), IFNγ (*B*), and FoxP3 (*C*) were then determined by flow cytometry. All error bars represent SEM. Statistical analysis was performed using two-tailed Student's *t* test (*$P < 0.05$; **$P < 0.01$).

(26). It must be noted, however, that a cognitive benefit of bryo-1 has not been established in humans, with a phase 2 trial in patients with Alzheimer's failing to meet its primary endpoint (9). Furthermore, differences in the character and pathophysiology of cognitive changes in MS versus other neurodegenerative conditions (such as Alzheimer's disease) makes the possibility of a similar benefit in patients with MS purely speculative.

In summary, we report here dramatic beneficial effects of bryo-1 in the EAE mouse model of MS, with cellular targets and in vivo actions potentially relevant not only to RRMS but also progressive forms of disease (primary progressive MS and secondary progressive MS). One major advantage of bryo-1 over other compounds tested in EAE is its extensive study in phase 1 and 2 clinical trials in cancer and Alzheimer's disease, which have demonstrated a favorable safety profile in humans (2–4, 9). Furthermore, oral formulations of the drug have been successfully employed in mouse models of Alzheimer's disease. As such, clinical exploration of bryo-1 in MS should be feasible in the future.

Materials and Methods

Reagents and Antibodies. Bryo-1 was purchased from Tocris (catalog #2383). $MOG_{35–55}$ peptide (amino acid sequence MEVGWYRSPFSRVVHLYRNGK) was prepared by the Johns Hopkins Synthesis and Sequencing Core Facility. Incomplete Freund's adjuvant was purchased from Thermo Scientific (catalog #77145), and complete Freund's adjuvant was prepared by adding 8 mg/mL heat-killed *Mycobacterium tuberculosis* H37 Ra (Difco, catalog #231141). Pertussis toxin was purchased from List Biologicals (catalog #181). LPS from *Escherichia coli* O55:B5 was purchased from Sigma (catalog #L6529). Flow antibodies against CD4 (46-0042-82), CD40 (17-0401-82), CD44 (47-0441-82), FoxP3 (12-5773-82), and IL-17a (17-7177-81) were purchased from eBioscience. Antibodies against IFNɣ (505806) and CD86 (105008) were purchased from Biolegend. All other pertinent reagents are described here.

Mice. Wild-type C57BL/6J mice were purchased from the Jackson Laboratory. All mice were housed in a dedicated Johns Hopkins mouse facility. All protocols were approved by the Johns Hopkins Institutional Animal Care and Use Committee.

Induction and Scoring of EAE. Active EAE was induced in 8–12 wk-old female C57BL/6J mice that had been allowed to acclimatize to the animal facility for at least 1 wk. $MOG_{35–55}$ peptide dissolved in PBS at a concentration of 2 mg/mL was mixed 1:1 with complete Freund's adjuvant (prepared as described earlier) to make an emulsion. On day 0, mice were immunized by injecting 50 μL of the emulsion s.c. into each of two sites on the lateral abdomen. In addition, on day 0 and again on day 2, mice were injected intraperitoneally with 250 ng pertussis toxin. Mice were weighed and scored beginning on day 7 postimmunization. Scoring was performed in a blinded manner according to the following scale: 0, no clinical deficit; 0.5, partial loss of tail tone; 1.0, complete tail paralysis or both partial loss of tail tone plus awkward gait; 1.5, complete tail paralysis and awkward gait; 2.0, tail paralysis with hind limb weakness evidenced by foot dropping between bars of cage lid while walking; 2.5, hind limb paralysis with little to no weight-bearing on hind limbs (dragging), but with some movement possible in legs; 3.0, complete hind limb paralysis with no movement in lower limbs; 3.5, hind limb paralysis with some weakness in forelimbs; 4.0, complete tetraplegia but with some movement of head; 4.5, moribund; and 5.0, dead.

Treatment of Mice with Bryo-1. Bryo-1 was prepared by initially dissolving in 100% ethanol and then further diluting to 20% ethanol and 1% DMSO in PBS. The final concentration of bryo-1 was 10 μg/mL Mice were treated by i.p. injection of 30 μg/kg bryo-1 or an equal volume of vehicle control (20% ethanol and 1% DMSO in PBS) 3 d per week (Monday, Wednesday, Friday). In one set of experiments, treatment began on the same day as immunization with $MOG_{35–55}$ (day 0). In a second set of experiments, mice were randomized and treatment was begun when the mice reached a clinical score of 1.0 (corresponding to tail paralysis). In this paradigm, mice received their first treatment on the day they reached a score of 1.0, and subsequently were returned to a 3 d/week schedule in sync with the other animals. In a third set of experiments, mice were randomized and treatment was begun on day 28 postimmunization, more than 10 d after peak disease and once motor deficits had reached a stable plateau.

Preparation of Bryo-1 for Treatment of Cultured Cells. For treatment of cultured cells, bryo-1 was dissolved in 100% ethanol to a final concentration of 20 μM, which was subsequently used for treatment. Ethanol alone was used as vehicle control.

Preparation of Mouse Tissue for Flow Cytometry. Mice were killed with pentobarbital and perfused via cardiac puncture with ice-cold HBSS without cations. Brain, spinal cord (collected using hydrostatic pressure), spleen, and lymph node tissue were isolated after perfusion and were mechanically dissociated by passing through 100-μm cell strainers. For CNS tissue, after dissociation, infiltrating mononuclear cells were separated from myelin debris using a 37/70% percoll gradient. After dissociation, spleens were incubated in ACK lysis buffer to remove red blood cell contamination. Cells were counted using a MACSQuant flow cytometer (Miltenyi Biotec).

Flow Cytometry and Intracellular Cytokine Staining. All staining procedures were performed in the dark at room temperature. For analysis of surface marker expression on bone marrow-derived DCs, cells were first stained with LIVE/DEAD aqua (Life Technologies, L-34966) for 30 min at room temperature in PBS. Fc receptors were blocked with anti-CD16/CD32 (Biolegend, 101320) for the final 10 min of staining. The cells were then washed and stained with specific conjugated antibodies for the specified surface markers in FACS buffer (PBS supplemented with 2% FBS and 1 mM EDTA) for 30 min.

For surface marker and intracellular cytokine staining of T cells, the cells were first restimulated with a cell stimulation mixture with protein transport inhibitors (eBioscience, catalog #00-4975-03) for 4 h in cRPMI at 37 °C. They then underwent live/dead and surface marker staining as earlier. For intracellular cytokine staining, cells were permeabilized and fixed using either IC Fixation buffer for cytokine analysis (eBioscience, 00-8222-49) or FoxP3 fixation/permeabilization buffer for transcription factor analysis (eBioscience, 00-5521-00) after manufacturer recommended protocol and incubated with specific conjugated antibodies for the specified proteins in permeabilization buffer for 1 h.

Cells were analyzed by flow cytometry using a MACSQuant flow cytometer (Miltenyi Biotec). Flow data analysis was performed in FlowJo (FlowJo) or FlowLogic (Inivai).

Preparation and Treatment of Murine BMDCs. BMDCs were generated as described (27), with minor modifications. Briefly, femurs were removed from 6–10-wk-old female C57BL/6J mice, cut on both ends, and marrow flushed with PBS. Bone marrow cells were then pelleted by centrifugation (500 × *g* for 8 min), resuspended in red blood cell lysis buffer (Sigma) for 1 min, and quenched with excess PBS. After another centrifugation, cells were resuspended in complete

RPMI (cRPMI) media consisting of RPMI-1640 with GlutaMAX supplement (Thermo Fisher Scientific) supplemented with 10% FBS, penicillin-streptomycin (Gibco), and 50 μM 2-mercaptoethanol (Sigma). On day 0, ~2×10^6 cells were then seeded per 100-mm plate in 10 mL media containing 20 ng/mL rmGM-CSF (Peprotech). On day 3, an additional 10 mL fresh cRPMI media containing 20 ng/mL rmGM-CSF was added to each plate. On day 6, half the culture supernatant from each plate was removed and centrifuged, and the pelleted cells resuspended in 10 mL fresh cRPMI with 20 ng/mL rmGM-CSF and added back to the plates. On day 8, all nonadherent cells (representing the BMDC fraction) were collected, pelleted by centrifugation, resuspended in fresh cRPMI media with 20 ng/mL rmGM-CSF, and plated into 24-well dishes. These BMDCs were then treated overnight with or without LPS 100 ng/mL plus the indicated doses of bryo-1. The following day (day 9), these cells were then assayed by flow cytometry or cytokine ELISA.

Preparation and Treatment of mPMs. Mice aged 8–12 wk were injected intraperitoneally with 2 mL each of 3% sterile thioglycollate (BD Biosciences, catalog #211716) medium. The mice were killed 3–5 d later, and cells were harvested by peritoneal lavage with ice-cold RPMI medium containing 2% FBS (FBS) and 1 unit/mL heparin. The cells were pelleted by centrifugation at 500 × *g* for 8 min, washed in ice-cold RPMI containing 2% FBS alone, pelleted by centrifugation, and resuspended in ice-cold Spinner-modification minimum essential medium (SMEM; Sigma, M8167) supplemented with 10% FBS, 2 mM glutamine, and penicillin-streptomycin (SMEM-complete). Cells were then counted, equal numbers were plated into each well of appropriate cell culture dishes, and the cells were then incubated at 37 °C for 2–4 h to allow macrophage adhesion. Contaminating nonadherent cells were then removed by washing culture dishes five times with ice-cold sterile PBS. Fresh SMEM-complete was then added to the plates, which were incubated overnight at 37 °C. The following day, the mPMs were treated for 24 h with vehicle, LPS 100 ng/mL, or IL-4 20 ng/mL plus the indicated doses of bryo-1 and then assayed by cytokine ELISA or Western blot.

ELISA. After overnight treatment of BMDCs or mPMs with LPS 100 ng/mL ± bryo-1, culture supernatants were collected and cytokine production was assayed using ELISA kits for IL-12 p70 (catalog #88-7121-22), IL-6 (catalog #88-7064-22), and IL-10 (catalog #88-7105-22) purchased from eBioscience, according to manufacturer's instructions. Plates were read at 450 nm on a tabletop plate reader.

Western Blotting. Cells were lysed by sonication in RIPA buffer supplemented with protease inhibitors, and protein concentration was measured by Bradford assay. Lysates were mixed with SDS sample buffer, boiled, and resolved by SDS/PAGE. Bands were transferred to PVDF Immobilon P membranes (Millipore) using a wet transfer, blocked in TBS-T containing 5% milk, and probed overnight at 4 °C with mouse monoclonal antibody against arginase -1 (Santa Cruz Biotechnology, catalog #sc-271430, 1:500). HRP-conjugated anti-mouse secondary antibody was from Jackson ImmunoResearch. Western blots were visualized using the SuperSignal West ECL system (Thermo Scientific), followed by film exposure. Blots were then stripped using Restore Western blot stripping buffer (Thermo Scientific, catalog #21059), blocked again as earlier, and probed overnight at 4 °C with HRP-conjugated anti-actin antibody before visualization as earlier. Quantitation was performed using ImageJ software.

Preparation of Naive $CD4^+$ T Cells. Spleens were harvested from 6–10-wk-old female C57BL/6J mice, and single-cell suspensions were generated in FACS buffer by disrupting spleens with the plunger of a syringe over a 70-μm nylon cell strainer (BD Falcon), pelleting cells by centrifugation (500 × *g* for 8 min), and resuspending in fresh FACS buffer. Naive $CD4^+$ cells were then isolated by negative selection using an isolation kit from STEMCELL Technologies (catalog #19765).

Stimulation of Naive $CD4^+$ T Cells with α-CD3/CD28 Antibodies. Tissue culture plates were coated with α-CD3 antibody (BD Biosciences) by incubating them with 0.25–1.0 μg/mL of antibody diluted in sterile PBS overnight at 4 °C or for 2–4 h at 37 °C. The antibody solution was then removed, plates were washed once with sterile PBS, and naive $CD4^+$ T cells (prepared as described earlier) were seeded along with 0.25–1.0 μg/mL α-CD28 antibody (BD Biosciences) in the presence or absence of the indicated doses of bryo-1. The cells were cultured for 3 d and then analyzed by flow cytometry.

Statistical Analyses. For comparison of clinical scores in EAE experiments, Mann–Whitney *U* test was performed. For all other statistical analyses, two-tailed Student's *t* tests were used. All error bars depict SEM.

ACKNOWLEDGMENTS. We are grateful to K. Whartenby for her insights and discussion. We thank B. Paul for providing the protocol for mPM isolation. Funding provided by the National Multiple Sclerosis Society, American Academy of Neurology, Conrad N. Hilton Foundation (M.D.K.), National Institutes of Health R37NS041435 (to P.A.C.), and National Institutes of Health 5R01 MH018501 (to S.H.S.).

1. Trindade-Silva AE, Lim-Fong GE, Sharp KH, Haygood MG (2010) Bryostatins: Biological context and biotechnological prospects. *Curr Opin Biotechnol* 21:834–842.
2. Clamp A, Jayson GC (2002) The clinical development of the bryostatins. *Anticancer Drugs* 13:673–683.
3. Clamp AR, et al.; Cancer Research UK Phase I/II Committee (2003) A phase II trial of bryostatin-1 administered by weekly 24-hour infusion in recurrent epithelial ovarian carcinoma. *Br J Cancer* 89:1152–1154.
4. Sun MK, Alkon DL (2006) Bryostatin-1: Pharmacology and therapeutic potential as a CNS drug. *CNS Drug Rev* 12:1–8.
5. Etcheberrigaray R, et al. (2004) Therapeutic effects of PKC activators in Alzheimer's disease transgenic mice. *Proc Natl Acad Sci USA* 101:11141–11146.
6. Nelson TJ, Cui C, Luo Y, Alkon DL (2009) Reduction of beta-amyloid levels by novel protein kinase C(ε) activators. *J Biol Chem* 284:34514–34521.
7. Hongpaisan J, Sun MK, Alkon DL (2011) PKC ε activation prevents synaptic loss, Aβ elevation, and cognitive deficits in Alzheimer's disease transgenic mice. *J Neurosci* 31:630–643.
8. Schrott LM, et al. (2015) Acute oral Bryostatin-1 administration improves learning deficits in the APP/PS1 transgenic mouse model of Alzheimer's disease. *Curr Alzheimer Res* 12:22–31.
9. PR Newswire (May 1, 2017) NEUROTROPE announces positive top-line results from phase 2 study of bryostatin-1 for moderate to severe Alzheimer's disease. Available at https://www.prnewswire.com/news-releases/neurotrope-announces-positive-top-line-results-from-phase-2-study-of-bryostatin-1-for-moderate-to-severe-alzheimers-disease-300448563.html. Accessed December 16, 2017.
10. Ariza ME, et al. (2011) Bryostatin-1, a naturally occurring antineoplastic agent, acts as a Toll-like receptor 4 (TLR-4) ligand and induces unique cytokines and chemokines in dendritic cells. *J Biol Chem* 286:24–34.
11. Kaisho T, et al. (2002) Endotoxin can induce MyD88-deficient dendritic cells to support T(h)2 cell differentiation. *Int Immunol* 14:695–700.
12. Marta M, Andersson A, Isaksson M, Kämpe O, Lobell A (2008) Unexpected regulatory roles of TLR4 and TLR9 in experimental autoimmune encephalomyelitis. *Eur J Immunol* 38:565–575.
13. Cohen SJ, Cohen IR, Nussbaum G (2010) IL-10 mediates resistance to adoptive transfer experimental autoimmune encephalomyelitis in MyD88(-/-) mice. *J Immunol* 184:212–221.
14. Weber MS, et al. (2007) Type II monocytes modulate T cell-mediated central nervous system autoimmune disease. *Nat Med* 13:935–943.
15. Dutta R, Trapp BD (2014) Relapsing and progressive forms of multiple sclerosis: Insights from pathology. *Curr Opin Neurol* 27:271–278.
16. Grigoriadis N, van Pesch V; ParadigMS Group (2015) A basic overview of multiple sclerosis immunopathology. *Eur J Neurol* 22:3–13.
17. Lassmann H, van Horssen J, Mahad D (2012) Progressive multiple sclerosis: Pathology and pathogenesis. *Nat Rev Neurol* 8:647–656.
18. Procaccini C, De Rosa V, Pucino V, Formisano L, Matarese G (2015) Animal models of multiple sclerosis. *Eur J Pharmacol* 759:182–191.
19. Steinman L, Zamvil SS (2005) Virtues and pitfalls of EAE for the development of therapies for multiple sclerosis. *Trends Immunol* 26:565–571.
20. Miron VE, et al. (2013) M2 microglia and macrophages drive oligodendrocyte differentiation during CNS remyelination. *Nat Neurosci* 16:1211–1218.
21. Church JS, Milich LM, Lerch JK, Popovich PG, McTigue DM (2017) E6020, a synthetic TLR4 agonist, accelerates myelin debris clearance, Schwann cell infiltration, and remyelination in the rat spinal cord. *Glia* 65:883–899.
22. Gonzalez GA, et al. (2016) Tamoxifen accelerates the repair of demyelinated lesions in the central nervous system. *Sci Rep* 6:31599.
23. Sun MK, Alkon DL (2014) The "memory kinases": Roles of PKC isoforms in signal processing and memory formation. *Prog Mol Biol Transl Sci* 122:31–59.
24. Sen A, Hongpaisan J, Wang D, Nelson TJ, Alkon DL (2016) Protein kinase Cε (PKCε) promotes synaptogenesis through membrane accumulation of the postsynaptic density protein PSD-95. *J Biol Chem* 291:16462–16476.
25. Sun MK, Hongpaisan J, Lim CS, Alkon DL (2014) Bryostatin-1 restores hippocampal synapses and spatial learning and memory in adult fragile x mice. *J Pharmacol Exp Ther* 349:393–401.
26. Chiaravalloti ND, DeLuca J (2008) Cognitive impairment in multiple sclerosis. *Lancet Neurol* 7:1139–1151.
27. Lutz MB, et al. (1999) An advanced culture method for generating large quantities of highly pure dendritic cells from mouse bone marrow. *J Immunol Methods* 223:77–92.